Effect of Multi-Axial Stress State on the Deformation Path in Tube Flaring Process By Necking Instability Criteria

Bruno Buchmayr (bruno.buchmayr@unileoben.ac.at)
University of Leoben https://orcid.org/0000-0002-4941-8390
Alireza Omidvar
University of Leoben

Research Article

Keywords: Formability, Multi-Axial Stress State, Tube flaring, Finite Element Simulation, Instability Necking Criteria

Posted Date: May 27th, 2021

DOI: https://doi.org/10.21203/rs.3.rs-566770/v1

Noname manuscript No.
(will be inserted by the editor)

Effect of Multi-Axial Stress State on the Deformation Path in Tube Flaring Process By Necking Instability Criteria

Bruno Buchmayr · Alireza Omidvar

Received: date / Accepted: date

Abstract Various parts for automotive, appliance and oil industry are produced from tubes that are assembled and welded. For gaining the best weight savings, durability and cost reasons (energy saving, production cost, etc) the formability of the tubular materials is very important. The overall success of deformation process heavily depends on the incoming tubular material properties. In this work, formability of tubular steels is experimentally characterized and with the development of a numerical model the effect of biaxial stress state has been investigated. An experimental method has been developed to characterize the importance of multi-axial stress state on the formability of tubes. This requires the deformation in form of flaring of the tubular samples through a conical die. Damage strains are determined with the help of Hill-Swift Sheet Metal Forming Criteria and a plot of main strains occurring during the tube flaring test, after variation of the die-angle and friction coefficient has been resulted. Experimental results were then entered into the damage models of finite element program DEFORM™-PC PRO and used to calibrate the damage model for formability so that a sizable variation of range of multiaxial state of stress could be produced. The results showed that with increasing the stress multiaxiality of tubular steels, the damage strain was reduced. This indicates that the proposed method could be used of benefit in quality control in the production of tubes specially in the monitoring and controlling of tubes production such as tube rolling, welding and annealing.

Keywords Formability · Multi-Axial Stress State · Tube flaring · Finite Element Simulation · Instability Necking Criteria

Bruno Buchmayr

E-mail: bruno.buchmayr@unileoben.ac.at Alireza Omidvar
Institute for Metal Forming, University of Leoben, Leoben, 8700, Austria
E-mail: aromidvar@outlook.com

1 Introduction

Tube formability material properties are required for the accurate design of components used in a wide range of applications such as steering wheel columns, spacecraft landing gear, brakes in trains and elevators and automotive crash tests. Tube formability may also be used in industrial applications such as tube reduction/expansion or pipe connectors. [1] One of the most important factors that affect the formability is the state of stress. Most of the resulting stresses subjected on engineering components are complex and it is not possible to experiment with each individual state of stress, therefore it is necessary to reduce these to one or two types which control plastic deformation. One of these states is measured through formability tests which cannot be defined by a single material property, but are a complex combination of several metallurgical and metal-forming parameters. "Formability" may be defined as the relative ease with which a metal can be shaped through plastic deformation before damage occurs. It is clear that the formability properties of tubes which are used in the design of the manufacturing process of tubular components are slightly different than the flat sheet from which a tube is rolled. This is because during roll forming and welding of tubes some of the formability of the tube blank sheet is consumed, thus the formability is different in comparison to the original sheet. Taking the advantage of the physical modelling, estimations are carried out, validated with damage criteria included in the finite element code as well as contours of multiaxiality and Load-stroke graphs of the upper-die during experimental forming of the tubes. Generally, the damage critical value can be defined by microscopic observation and mathematical methods as Normalized C&L, McClintock and Rice & Tracy [4].

The rest of this paper is organized that the theoretical background and the experimental method for the deformation of the tubes are the subject of sections 1 and 2. Experimental setup are discussed thoroughly in section 3 and section 4 represent the results of experiments. The Finite Element modeling results along with the experiments discover the Forming Limit Diagram used for analyzing the tube deformation path in Section 5.

Finally in section 6 the effect of different stress states on the deformation of the tubes are summarized and the results are compared and possible further work on this topic will be discussed.

2 Theoretical Background

Basically, ductile failure results from too severe plastic deformation. Damage may be interpreted on the microscale as breaking of atomic bonds and plastic enlargement of microcavities. On the macroscale the number of microcavities may be approximated by introducing a scalar parameter, say D, to quantify the material damage process. [7]

In the past several different approaches were developed and applied to the analysis of ductile fracture. However, the connection between failure and deformation is complicated. An important connecting mechanism is seen to be the development of internal damage, the local loss of coherency due to voids, etc.: large plastic deformation causes internal damage and a critical amount of internal damage is necessary to represent a micro-crack. Thereby, the local internal damage may affect the overall flow behavior of the material. This, as well as its possible technical application in predicting crack-initiation has been studied extensively. The concept of a critical amount of some accumulative quantity, like internal damage, results in a number of empirical failure criteria. The most quoted ones are that by Cockcroft and Latham and that by Oyane, as presented in the literature. [4, 5, 8, 11, 14, 15, 18]

All these criteria state some quantity to have a constant value at failure, independent of the triaxiality path.

The data presented on the table 1 shows that the Cockcroft and Latham criterion was not satisfying, with respect to its invariancy. With respect to the three critical density criteria showed above, only the one with an exponential relationship between void growth rate and triaxiality is applicable. The first one is a modification of the specific plastic work criterion. The second criterion belongs to a class that states that failure occurs after a critical density change such as void growth equation of Rice and Tracey proposed by Lemaitre.

Table 1 Comparison of several damage criteria [17]

Criteria	Invariancy of constant C (experiment)	Equation	Comment
Cockcroft and Latham	Not satisfying	$C_1 = \int_0^{\varepsilon_f} \frac{\sigma_1}{\bar{\sigma}} d\bar{\varepsilon}$	Modification of plastic work
Oyane	Underestimate the effect of high triaxiality	$C_2 = \int_0^{\varepsilon_f} (1 + A\frac{\sigma_m}{\bar{\sigma}_f}) d\bar{\varepsilon}$	Critical density change
Rice and Tracey	Satisfying over whole range of tests	$C_3 = \int_0^{\varepsilon_f} exp(\alpha \frac{\sigma_m}{\bar{\sigma}})\, d\bar{\varepsilon}$	Critical density change
Lemaitre	Restricted to the ferro metals	$\left(\frac{\bar{\Sigma}}{\sigma_y}\right)^2 + 2f_v\, cosh(\frac{3}{2}\frac{\Sigma_m}{\sigma_y}) - (1 + f^2) = 0$	Critical density change

According to the Rice and Tracey, proved to be reasonably satisfying over the whole range of multiaxiality ratio as well as all the metal which has been tested. This provided that the criterion is optimized, with respect to the invariancy of C_3 in

$$C_3 = \int_0^{\varepsilon_f} exp(\alpha \frac{\sigma_m}{\bar{\sigma}})\, d\bar{\varepsilon} \quad (1)$$

by varying the parameter α. The optimal value for α is quite similar for low carbon steels 1045, 1022 and non-ferrous metals. It suggests that the value of 3/2 for the factor in the exponential term is too large. Indeed, a lower value of 1.03 provides better results and indicates a similarity in the effect of the multiaxiality on the failure behavior of these steels. [17]

2.1 Rice & Tracey Damage Criteria

According to the criteria Rice and Tracey shown in Table 2 having applied the uniaxial case results.

$$\sigma_1 \neq 0, \sigma_2 = \sigma_3 = 0. -\frac{3}{2}\frac{\sigma_m}{\bar{\sigma}} = -\frac{1}{2}, exp\left(-\frac{1}{2}\right) = \frac{1}{1.65} \quad (2)$$

One can now define the constant value and calculate the damage strain in the triaxial case which is related to the critical strain„ in a uniaxial case as follows:

$$\varepsilon_f = 1.65\varepsilon_0\, exp\left(-\frac{3}{2}\frac{\sigma_m}{\bar{\sigma}}\right) \quad (3)$$

Analyzing the comments on damage criteria which have been proposed it appears to be much more justified to apply the damage model whose results are more reliable and in addition are comparable with damage micromechanics as detailed in the work of Rice and Tracey. [4]

The critical values at fracture C_i are usually obtained for each ductile fracture criterion directly from the strain paths, can be define as a function of the

material. It must be noted that the integration of the left-hand side of each criterion is the damage which the material has during plastic deformation (refer to Table 1). Obviously, different critical values at fracture,C_i, are found for each ductile fracture criterion. [8]
For getting a good and reliable results damage values calculated in modeling are compared with the distribution of damage-value at the location of the fracture in tube sample. Then if the maximum values are located at the crack area this could be taken as critical values of damage. Finding out the critical damage value, different stress states can be evaluated for the same material. Previous chapters showed some concepts concerning damage models in general and in the next chapters the effect of stress state on metal failures more specifically are shown and the constitutive relationships between stress state and damage strain are theoretically analyzed.

2.2 Relationship of fracture limits and multiaxiality

Multiaxiality can result in tubes by application of the plane-stress state on tube specimens($\sigma_3 = 0$). These could be studied via a combination of compression and tension during tube deformations. Therefore, material data for tube formability must be obtained by deforming tubular samples under a biaxial state of stress. Process simulations are used for a reverse analysis method in which experimental results are input into the simulations and the required materials property such as the relation between flow stress and strain (flow curve), the friction coefficient μ and the strain hardening exponent, n, must be accurate.
In order to present the plot of forming limits as a function of multiaxiality, different multiaxial stress states are required which allow the φ -value (multiaxiality) to vary differently. It should be noted that the φ -value is the ratio of the hydrostatic stress (σ_m) to the equivalent stress ($\bar{\sigma}$) as shown in equation 4.

$$\varphi = \frac{\sigma_m}{\bar{\sigma}} \quad (4)$$

The multiaxiality ratio plays a very important role in the rupture of materials and makes materials brittle as it increases [7]. Considering the plane stress the following equation is attained.

$$[\sigma] = \begin{bmatrix} \sigma_1 & 0 & 0 \\ 0 & \sigma_2 & 0 \\ 0 & 0 & 0 \end{bmatrix} \quad (5)$$

from the plastic incompressible condition, it follows that:

$$[\varepsilon] = \begin{bmatrix} \varepsilon_1 & 0 & 0 \\ 0 & \varepsilon_2 & 0 \\ 0 & 0 & -(\varepsilon_1 + \varepsilon_2) \end{bmatrix} \quad (6)$$

rupture plastic strain P_R may be calculated as a function of the strain components, then:

$$P_R = \left(\frac{2}{3}\varepsilon_{ij}\varepsilon_{ij}\right)^{1/2} = \frac{2}{\sqrt{3}}\left({\varepsilon_1}^2 + {\varepsilon_2}^2 + \varepsilon_1\varepsilon_2\right)^{1/2}. \quad (7)$$

From the master curve of ductile fracture in the case of plane stresses, neglecting elastic strain and assuming proportional loading gives the result:

$$P_R = \varepsilon_R \left[\frac{2}{3}(1+\nu) + 3(1-2\nu)\left(\frac{\sigma_m}{\bar{\sigma}}\right)^2\right]^{-1} \quad (8)$$

where ν =Poisson Ratio and ε_R = rupture strain.
Plastic deformation is mainly related to the slip process which does not depend on the hydrostatic stress. It is clear from equation (8) that damage is influenced by hydrostatic stress or the multiaxiality ratio. Furthermore, assuming no kinematical hardening and proportional loading, it is straightforward to show the proportionality between strain and components of the deviatoric stress:

$$\frac{\varepsilon_1}{\varepsilon_2} = \frac{\sigma_2^D}{\sigma_1^D} \quad (9)$$

where σ_1^D and σ_2^D are deviatoric stresses.
from which it follows that:

$$\frac{\sigma_m}{\bar{\sigma}} = \frac{\frac{\varepsilon_2}{\varepsilon_1}+1}{\sqrt{3}\left[\left(\frac{\varepsilon_2}{\varepsilon_1}\right)^2 + \frac{\varepsilon_2}{\varepsilon_1}+1\right]^{1/2}} \quad (10)$$

Replacing ε_1 and ε_2 from experiment results of the ring expanding test in

equation 7, 8 and 10 we can calculate the interdependence of state of stress ($\frac{\sigma_m}{\bar{\sigma}}$) and rupture strain ($\varepsilon_R$).

$$\varepsilon_R = \frac{2}{\sqrt{3}}(\varepsilon_1{}^2 + \varepsilon_2{}^2 + \varepsilon_1\varepsilon_2)^{1/2}\left[\frac{2}{3}(1+\nu) + 3(1-2\nu)\left(\frac{\sigma_m}{\bar{\sigma}}\right)^2\right] \quad (11)$$

3 Tube Flaring Experimental Setup

This is a designed experiment to determine the effect of multiaxiality on the formability of tubular materials (referred to as tube expansion). This tube expansion test has been originally taken from European standard Ref.-Nr. EN 10236: 1993 D[23] and allows formability tests on the tubes.

Figure 1. Tool's set of ring expanding test

A cone-shaped punch is undertaken for enlarging a cylindrical ring to its open side. The ring samples are supported on the opposite side with a thicker tube. As the punch presses into the ring, along the axis of rotational symmetry, the tube walls are forced to expand in the circumferential direction and for fulfilling the volume conservation in plastic deformation, the plastic straining in the circumferential direction has to be consumed for by a reduction of the wall thickness and a retraction of the material in axial direction. The material retraction causes the expanded section of the cylinder to be shorter than any simple bending deformation mode [18]. This continues until a crack initiates and propagates thoroughly that are used to determine the limits of tubular material.

The experiments were carried out using a 1000 KN computer-controlled hydraulic press with a slow strain rate which has a velocity of 7 mm/s. Referring to Fig. 1, the tools consists of a set of conical punch with angles of α=45° and α=30° , punch holder plate, tube fixing plate so that the ring and supporting tube can be placed on them, switches for turning off/on and controlling the direction of ram movement and PC controller with a interface to the press load cell to record and store the measured data.

In order to allow load recording during experiments, the force was applied to the punch and was measured by a single load cell under the fixing plate. A PC-based data logging system which is connected to the AD-DA transducer of the load cell was used to record and store loads and displacements so that it could be analyzed later on. For gaining better results comparable with the simulation and with several possible friction coefficients, the samples were lubricated with PTFE Teflon, automobile grease and deep drawing lubricant on the inner side of the tube and the outer surface of dies.

The upper conical die was turned from a CK45 steel rod and hardened at 820˚C for ¾ hour and quenched in 75˚C oil to reach 54 HRC. It was also held by the upper plate with four M24 standard screws which was fixed to the

center axis of upper ram of the press. On the lower side the ring support and the ring specimen are fixed in place between a ring with diameter equal to the inner diameter of the tube and a plate called fixing plate with a hole in its center equal to the outer tube diameter. As the oil pressure reached steady state, the holder began to push the upper ram into the tube to perform the tube flaring process. For evaluating the mechanical behavior of tubes, it is supposed that the experiment should be continued until the whole tube length was consumed by progressive buckling or necking.
All samples are measured in the end length and diameter so that the strain limits could be derived. The graphs of tool stroke depth versus the force driving the tool are also resulted that are later used for finite element simulation. Both data are investigated by means of finite element method. Several samples were cut from 6 m long tube of structural steel St 52-3 and stainless steel 316. The samples have a thickness of 2.5 mm and 2 mm and outer radius of 35 mm and 38.1 mm. In practice these short cylinders had to be supported by a thicker tube for an effective constraint in axial direction. For every single test both a tube and support were needed. One should minimize the buckling effect in order to gain the forming limits of tube expansion. for preventing the buckling of tubes, the length-to-diameter ratio was reduced from 1.5 to 0.5.
Afterward the rupture strain namely in the circumferential and longitudinal directions were measured. Using this as a reference the damage model of the Simulation could be calibrated. In the simulation the critical value of damage can now be predicted with higher accuracy.
This means that the Finite Element simulation for the tube expansion with the same friction and geometry conditions will be conducted until the circumferential strain of the measured value from the experimental data is reached.
Finally, the location of the maximum damage value can be compared with the fracture site. If the maximum damage value location is at the same position of the fracture site, the results are reliable and good, so then the maximum damage value at the fracture point will be the critical damage value D_c of testing tube material. Otherwise, the applied ductile fracture criterion is inaccurate.

Even though the tension test was not suitable for the tube application, material data obtained from tensile test can still determine the flow curves of tubular material as the results are used later in the modeling of tests. For this reason, standard samples similar to the standard DIN EN 10002-1 B have been prepared. The maximum load was 250 kN and the ram velocity varied between 0.0005 and 600 mm/min. Both were controlled with a computer interface. To get better results from four specimens, two specimens were annealed at 820°c for 45 min and cooled in the air. Measured thickness and length of the samples with the data gained from a displacement sensor and load cell were imported into Zweck 250 software and imported for further analysis.

The mechanical properties of tube wall material are listed in table 2.

Table 2. Mechanical properties of st-52 tubes

Sample status	**E (GPa)**	**UTS (MPa)**	**σ_y (MPa)**	**%RA**	**K (MPa)** *	**n****
as received	14.7	436.69	359.40	0.173	668.4	0.19
Annealed	14.1	403.57	296.00	0.329	877.2	0.40

*k Stiffness coefficient **n Work hardening coefficient

The value 3/2 for k is mostly too high and for getting good results should be replaced with the value driven by the experimental results. These values listed in Table 2 and additional mechanical properties of tubular material were used for the estimation of Rice and Tracey coefficient which was defined theoretically 1.5 as well as direct application of the flow curves in the modeling in Deform program.

4 Results

The process of flaring of a tubular sample over a cone-shaped die is influenced by several parameters including angle of die, coefficient of friction between the die and the tube interface, geometrical parameters of the tube namely thickness and diameter, mechanical properties of the tube material and the velocity of the punch ram. Of the said parameters, the effect of die angle and the friction between the tube and die interface on the force-displacement or energy absorbing capacity of the flared tubes have been studies.
The results of the experiments were in the form of the Force-stroke diagram, forming limits of tubes and stress-strain relationship. Table 3 shows the experimental method which were used to vary the process parameters.

Table 3 Designed Experimental parameters for St 52 Tube Flaring Test

Item number	Die angle/Lubrication	Support (mm)	Length (mm)	Diameter (mm)
3/1	30 / Grease	70	35	70
4/1	45 / Grease	70	35	70
4/2	45 / without lubricant	70	35	70
4/3	45 / PTFE	70	35	70

A clear characteristic of the force-displacement diagram for the tube flaring experiment can be observed in figures 2. Between the elastic limit load and a displacement of 10 mm of the die, the driving force remains constant in 15 kN. This regime of higher value of 71.6 mm when no lubricant has been applied and decreased to 60.6 mm in the case of grease lubricant.
But the difference here within is that the instability points of the diagram changes to the lower value in the form of fracture rather than buckling or distortion.

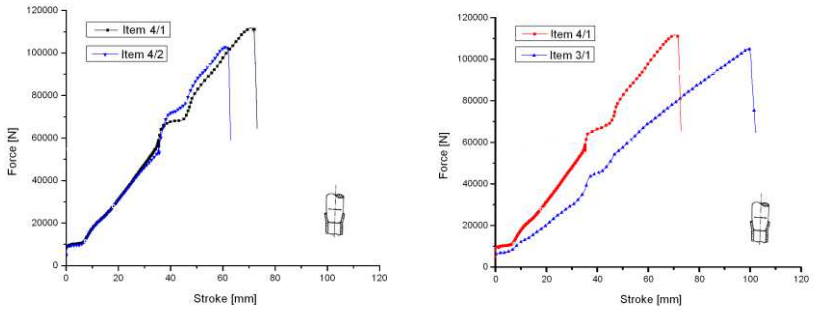

Fig 3 Effect of the friction and Die Angle on the force-stroke diagram (Item 4/1 Grease, Item 4/2 without lubricant, Item 3/1 α=30º, Item 4/1 α=45º)

The increasing of the die angle caused the force-displacement curves to shift slightly upward and left. Therefore, it can be argued that the deformation of the tube with the die profile is more easily obtained when the die angle is smaller and vice-versa. The following graph (Figure 4) has been used to estimate the friction coefficient which will be later applicable to Finite Element Method. Accordingly, the best curve for which fitted to the results obtaining by experiment was $\mu = 0.1$ for lubricant PTFE (blue curve), $\mu = 0.3$ when applied without lubricant (green curve).

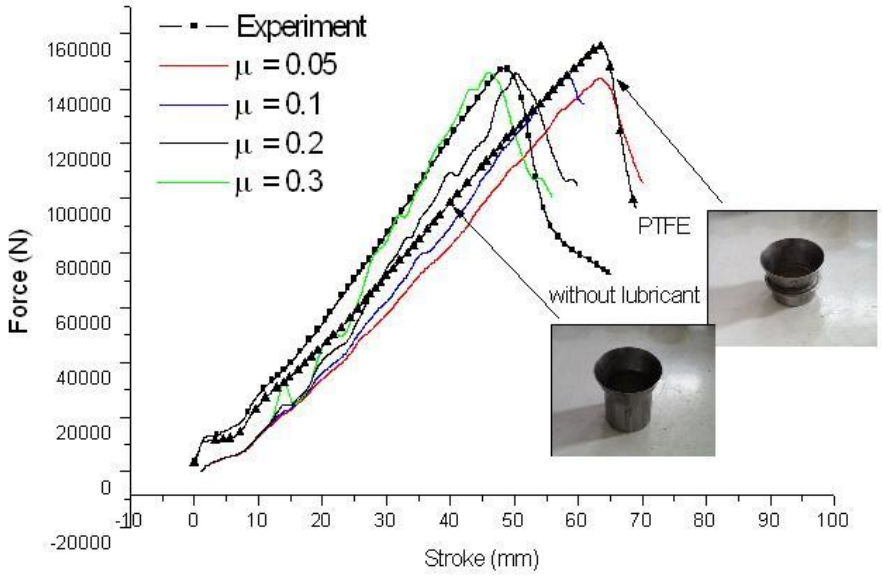

Figure 4 Data calibration for the estimating of friction coefficient

For gaining the FLD of tubular material hill and swift necking criteria for different multiaxiality ratio applied. Table 4 shows the measured and calculated value of strain limits in main directions:

Table 4. Forming limits of tubular materials * first four item distorted

				ε_1		ε_2		ε_3	
Item number	**Peak Stroke (mm)**	**End Diameter (mm)**	**End Length (mm)**	**measured**	**computed**	**measured**	**computed**	**measured**	**computed**
3/1	99.82	111	28.5	0.39	0.427	-0.18	-0.227	-0.21	-0.200
4/1	70.74	113	29.2	0.48	0.471	-0.18	-0.230	-0.30	-0.241
4/2	60.61	108	30.3	0.43	0.410	-0.14	-0.204	-0.29	-0.206
4/3	74.65	114	27	0.49	0.493	-0.23	-0.241	-0.26	-0.252

The results presented hereby with the deformation paths accordingly. The strain hardening exponent and sheet anisotropy were gained from tensile test and were used into the models.

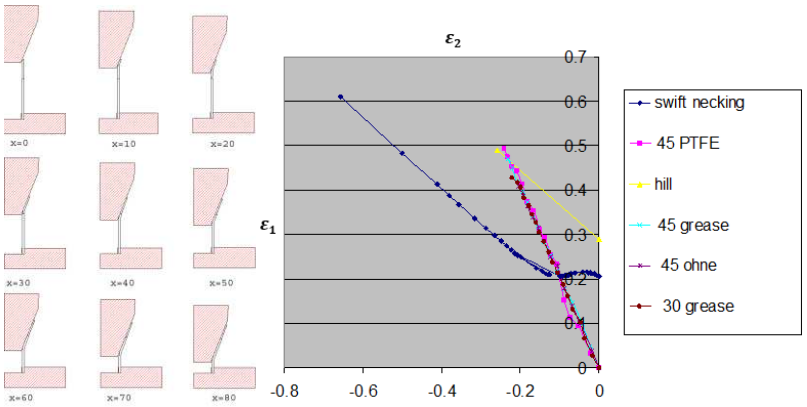

Figure 5. Forming Limit Diagram and related Simulated Deformation Path

Table 5 shows the values of strains for different deformation path. These values gained directly from the calculation from FEM software Deform. The graphical representation of the deformation scheme along with the forming limit diagram path are shown in figure 5.

Table 5. Deformation path until the material rupture of St 52-3

Stroke (mm)	PTFE, α=45°		Grease, α=45°		Dry, α=45°		Grease, α=30°	
	ε_1	ε_2	ε_1	ε_2	ε_1	ε_2	ε_1	ε_2
0	0	0	0	0	0	0	0	0
5	0.033	-0.021	0.048	-0.022	0.04	-0.018	0.027	-0.016
10	0.093	-0.052	0.098	-0.042	0.1	-0.048	0.067	-0.036
15	0.113	-0.072	0.148	-0.067	0.14	-0.068	0.102	-0.046
20	0.153	-0.089	0.178	-0.087	0.18	-0.089	0.131	-0.066
25	0.233	-0.107	0.218	-0.107	0.23	-0.106	0.161	-0.079
30	0.253	-0.122	0.253	-0.122	0.25	-0.123	0.187	-0.091
35	0.293	-0.137	0.283	-0.139	0.285	-0.14	0.213	-0.105
40	0.313	-0.152	0.318	-0.155	0.315	-0.154	0.237	-0.117
45	0.353	-0.167	0.343	-0.169	0.34	-0.168	0.26	-0.127
55	0.373	-0.182	0.373	-0.183	0.364	-0.182	0.283	-0.139
60	0.413	-0.196	0.397	-0.195	0.387	-0.192	0.305	-0.151
65	0.443	-0.208	0.418	-0.208	0.41	-0.204	0.326	-0.161
70	0.453	-0.22	0.45	-0.22			0.345	-0.17
75	0.473	-0.232	0.471	-0.23			0.364	-0.179
80	0.493	-0.241					0.383	-0.19
85							0.405	-0.198
90							0.416	-0.206
95							0.427	-0.221
D_c	1.25		1.19		1.04		1.08	
ε_f	0.50		0.50		0.41		0.43	

The profile of σ_m and $\bar{\sigma}$ for tube are shown in figure 6 that in the both case the maximum value of multiaxility-value occurs at the left corner of the ring (line K in profile) in which supposed that the crack are propagated from this location.

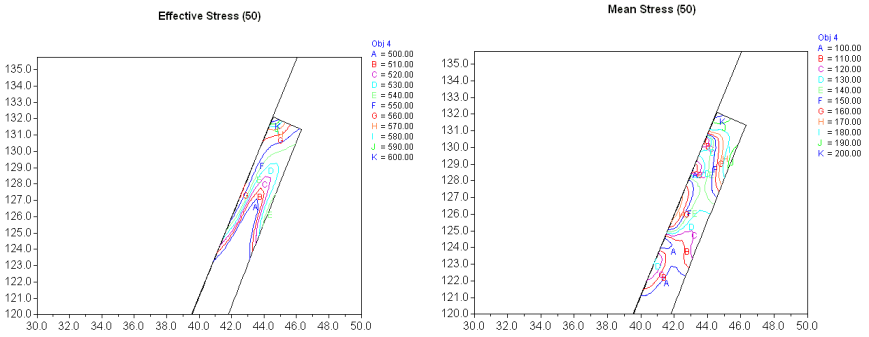

Figure 6. Profile of effective and mean stress

Furthermore the $\varphi = \frac{200}{600} = \frac{1}{3}$ multiaxial ratio are resulted which are constant in the all the simulation steps. The aggregated amount of triaxiality are shown in Table 4 with the effect of die angle and friction in which the value of $\varphi = \frac{1}{3}$ still remains unchanged if it is repeated. On the other hand, the damage critical value resulting from the experiment (Section 3) and constant k (Material Constant) calculated from section 4was substituted in the damage model Rice and Tracey of program. These data had a good agreement with the work of Rammerstorfer [18] and numerical results.

5 Discussion

Throughout this work, formability experiments have been used to describe the metal forming process whereby the tubes were formed into conical shapes with a die using a hydraulic press in which the variation of die angle, tubular materials and lubricant has been considered. Different manufacturing options namely seamless stainless steel and welded structural tubes were tested and the fundamental theoretical and numerical investigations on the instability of thin-walled cylinders were performed to find the bursting force.
It was presented that greater the angle of die, the greater the fracture strain in the circumferential and axial directions. With die of semi angle of 30° it was resulted to fracture strain of 0.4 as with the same metal forming condition with 45° die angle a fracture strain of 0.5 was resulted.
Seamless stainless-steel tubes showed a better formability as welded structural steel when the length of the tubes was short enough to avoid the buckling and distortion of the tubes. In addition, the experimentation of different lubricants was carried out. In case of insufficient lubricant, low fracture strain of 0.4 were obtained. With proper lubrication, PTFE or grease, it was observed that the fracture strain increased to value 0.5.

At last, a numerical study carried out assuming that the materials behave anisotropic. As result the deformation path, convenient damage model and calibration of coefficient of friction obtained. Comparison of numerical and experimental results indicated good agreement when stress-strain properties of tubular material obtained from simple tensile test were used in calculations. A note on calibration of the damage model of Rice and Tracey has been used and the graph of force-displacement showed a good agreement between FEM results and experiment. This calibration which has been applied resulted to estimation of the k-value. As result the relation between multiaxiality and damage effective strain (Stenger diagram) of tubular material obtained. With increasing the value of multiaxiality the deformabilty decreased exponentially. This results to determination of FLD of tubes. For gaining the FLD of tubular material hill and swift necking criteria for different multiaxiality ratio applied. The results presented hereby with the deformation paths accordingly. The strain hardening exponent and sheet anisotropy were gained from tensile test and were used into the models.
Finally, it should be noted that the prediction of accurate results in the area of formability in term of producibility can now obtain with the help of new technology of FEM and usage of high-tech instrumentation for controlling of process parameters.

References

[1] Daneshi G.H., Poorheydari-Anaraki K.. *Inversion of thin-walled tube under uniaxial loading* , 1st Conference of Iranian metallurgical engineering society, 1997.

[2] Homepage of Aristo Machines, Inc. 2003-2004 http://www.aristomachines.com/

[3] Goodall W., Skelton R.P., *The importance of multiaxial stress in creep deformation and rupture* , Fatigue Fract Engng Mater Struct 27, 267-272, 2003.

[4] Rice J.R., Tracey D.M., *On the ductile enlargement of voids in triaxial stress fields* , Mech. Phys. Solids 17, 201-217, 1969.

[5] Fischer F.D., Kolednik O., Shan G.X., Rammerstorfer F.G., *A note on calibration of ductile failure damage indicators*, International Journal of Fracture 73, 345-357, 1995.

[6] Johnson W., Mellor P.B., *Engineering plasticity*, 1983.

[7] W.L. Hu, Z.B. He, Y. Fang, *Uniform principle on stress, strain and yields locus for analyzing metal forming processes: the contribution of Prof. Z.R. Wang*, Journal of Materials Processing Technology 151, 27-32, 2004.

[8] Jean Lemaitre, *A Course on Damage Mechanics*, 1992.

[9] P.A.R. Rosa, J.M.C. Rodrigues, P.A.F. Martins, *External inversion of thin-walled tubes using a die: experimental and theoretical investigation*, International Journal of Machine Tools & Manufacture 43, 787-796, 2003.

[10] Syrikanth Kulukuru, Yingyot Aue-ul-lan, Taylan Altan, *Determining flow stress of tubes, Biaxial test provides better results for hydroforming*, TPJ Tube & Pipe Journal, March 12, 2002.

[11] Taylan Altan Hyunkee Kim, Masahito Yamanaka, *Prediction and elimination of ductile fracture in cold forgings using FEM simulations*, Proceedings of NAMRC Houghton, Michigan, Society of Manufacturing Engineers, 65-66, May 1995.

[12] Dipl. Ing. Bernhard Buchner, *Beurteilung der Umformbarkeit von Blechen durch die Ermittlung von r-Wert und n-Wert*, Übungen zu Umformtechnik und –mascheine II, Leoben, Lehrstuhl für Umformtechnik im Department of Product Engineering, 8-11, SS 2005.

[13] *Deform^{TM}-PC PRO NT/2000 User Manual*, Scientific Forming Technologies Corporation,Columbus,Ohio.

[14] Schuelter, F. Grimpe, W. Bleck,W. W. Dahl, *Modelling of the damage in ductile steel*, Computational Materials Science,7, 27-33 (1996).

[15] Rudolf Schiffmann, *Experimentelle Bestimmung der Schädigung und Modellmäβ ige Beschreibung der Schädigung beim Gleitbruch von Stählen*, Berichte aus dem Institut fuer Eisenhuettenkunde, RWTH Aachen,
16-22, 2001.

[16] Reiner Kopp, Herbert Wiegels, *Einfürung in die Umfortechnik*, Institut für Bildsame Formgebung, RWTH Aachen, 132-134, 1999.

[17] Pieter Jan Bolt, *Prediction of ductile fracture*, Department of Mechanical Engineer- ing, Technical University of Eindhoven, 96-120, 1989.

[18] T.Daxner, F.G. Rammerstrofer, F.D. Fischer, *Simulation of material and structural instability phenomena during the flaring process of cylindrical shells*, Computer Methods in Applied Mechanics and Engineering, 1-13, 2005.

[19] Thomas B. Stoughton, Xinhai Zhu, *Review of theoretical models of the strain-based FLD and their relevance to the stress-based FLD*, International Journal of Plasticity 20, 1463-1486, 2004.

[20] G. Nefussi, A. Combescure, , *Coupled buckling and plastic instability for tube hydroforming*, International Journal of Mechanical Science 44, 889-914, 2002.

[21] T.Daxner, F.G. Rammerstrofer, F.D. Fischer, *Instability phenomena during the conical expansion of circular cylindrical shells*, Computer methods in applied mechanics and engineering and , P 1-13, 2005.

Author biography

Bruno Buchmayr was born on March 17, 1954 in Leoben, Austria. He has received his Diploma Engineering from the University of Leoben and simultaneously worked for the Applied Mathematics Institute as a study assistant, when he completed his PhD. He was a guest fellowship at McMaster University in 1988 and was honored the Venia Legendi for Materials Science and Welding Technology at the Graz University of Technology when he was led the Christian Doppler Lab. In 1997 he became a.o. Univ.-Prof. at the Institute of Materials Science, Welding Technology and Chipless Forming Processes. He has played a decisive role as a key researcher since 1999 in the Computer Modelling Center of Virtual Automotive vif at Graz University of Technology. On February 1 , 2003 Bruno Buchmayr was dominated as the Professor and Chairman of Metal Forming Institute and continue his scientific focus to the area of Simulation, Material Properties and Manufacturing in the field of Metal Forming. He brought concept of 3D printing for Metals and tried to anchor digitization at the University of Leoben. As for more than 15 years membership of Christian Doppler Research Institute, Austrian Society for Metallurgical Engineering and advisory role in the Federal Ministry with regard to the "Manufacturing for Future" he has more than 240 publication , with the organization of international Conferences, was honored for numerous prizes such as Hans-Malzacher, Masubuchi-Shinso Corp, American Society for Welding, Franz-Leitner, ASM European Lecturer, Fellow ASM and Research Prize of the State of Styria.

Alireza Omidvar received the B.S degree in Materials Science and Engineering from Tehran Polytechnic University, Tehran, Iran (1999) and the M.S Degree in Metallurgical Engineering from the University of Leoben, Austria (2006). He has an extra Master Degree in System Engineering and Management (2018) from Industrial Management Institute, member of Management House in Industrial Management Institute branch of IDRO, Industrial and Development Renovation Organization, Tehran, Iran. With more than 10 years of working Experience in the Advanced Manufacturing System and related Organizations and Research Institutes.

He is a PhD candidate in Mechatronics of Artificial Intelligent Systems with Data Mining and Supply Chain Management.